DETECTION OF GROUPS OF CONCOMITANT EXTREMES USING CLUSTERING

V. FOMICHOV AND J. IVANOVS

ABSTRACT. There is a growing empirical evidence that the spherical k-means clustering performs remarkably well in identification of groups of concomitant extremes in high dimensions, thereby leading to sparse models. We provide first theoretical results supporting this approach, but also identify some pitfalls. Furthermore, we develop a novel spherical k-principal-components clustering algorithm which is more appropriate for identification of concomitant extremes. Our main result establishes a broadly satisfied sufficient condition guaranteeing the success of this method, albeit in a rather basic setting. Finally, we illustrate in simulations that k-principal-components outperforms k-means in the difficult case of weak asymptotic dependence within the groups.

1. Introduction

Statistical analysis of high-dimensional data typically relies on various sparsity assumptions, unless structural domain knowledge is available. In the study of extremes sparsity is especially important since the number of extreme observations is small by definition. The recent survey [Engelke and Ivanovs, 2020] reviews different notions of sparsity and the available tools in the context of extreme value statistics. Fundamental here is the notion of concomitant extremes [Chautru, 2015, Goix et al., 2016], where the focus is on the groups of variables which can be large simultaneously while others are small. Importantly, extremal dependence can be modelled separately in these groups and then combined into a mixture model, thereby leading to dimension reduction.

Mathematically speaking, our interest is in the identification of the lower dimensional faces of \mathbb{R}^d_+ charged with mass by the so-called exponent measure. Alternatively, we may look at the faces of the positive simplex charged with mass by the angular (spectral) probability measure. This task, however, is highly non-trivial since only approximate angles coming from a pre-limit distribution can be obtained in practice, and these normally lay in the interior of the simplex. Various approaches to the identification of concomitant extremes and respective maximal sets have been explored in the literature, see [Goix et al., 2016, Goix et al., 2017, Simpson et al., 2018, Chiapino et al., 2019, Meyer and Wintenberger, 2019]. The main idea is to use a certain neighbourhood of a given face and to assign the respective mass to this face. The simplest method [Goix et al., 2016] amounts to thresholding the entries of the rescaled extreme observations. Apart from being very sensitive to threshold choice this method is not applicable in higher dimensions [Goix et al., 2017], as it produces a large number of faces with few corresponding observations. Certain grouping of faces as suggested by [Goix et al., 2017] and [Chiapino et al., 2019] may be helpful, but it is still limited to moderate dimensions.

Key words and phrases. Angular measure; concomitant extremes; dimension reduction; principal components; spherical clustering.

A different approach to the identification of concomitant extremes was proposed by [Chautru, 2015], and it amounts to the spherical k-means clustering [Dhillon and Modha, 2001] of the approximate angles. Each centroid is then attributed to a certain face by thresholding. Consistency of the spherical clustering has been recently established by [Janssen and Wan, 2020], who also provided further numerical illustrations. This approach has also led to useful and interpretable results for a real world 68-dimensional dataset in the review paper [Engelke and Ivanovs, 2020]. Finally, our problem is very different from those addressed by subspace clustering techniques for high-dimensional data [Gan et al., 2007, Ch. 15], which are popular in computer science.

Clustering in detection of concomitant extremes may seem intuitive to some extent, and there is a growing evidence that it performs extremely well in high dimensions comparative to other methods. The drawback is that there is no theoretic evidence of the efficacy of this method. The only theory available is the consistency result by [Janssen and Wan, 2020], but that is only marginally related to concomitant extremes. In this work we provide some basic theory showing that this procedure must work in certain cases indeed. Importantly, the k-means type of spherical clustering is not the best in terms of viable theoretical results, neither it is supported by simulations. We propose a spherical k-principal-components clustering arising from an alternative cost function. The name derives from the fact that the Perron–Frobenius eigenvectors of certain non-negative definite matrices with non-negative entries are used instead of the means in the updates of the algorithm. Interestingly, these matrices are the analogues of the cross-moments matrix used by [Cooley and Thibaud, 2019] and [Drees and Sabourin, 2019] in their principal component analysis of extremal dependence, whereas the bivariate case has been considered by [Larsson and Resnick, 2012] in another context.

Our main result in Theorem 5.2 provides a sufficient condition guaranteeing the success of the k-principal-components clustering in detection of concomitant extremes, albeit in a rather basic setting. Importantly, k-means fails in some fundamental cases, whereas k-principal-components is much more robust. Our counterexamples provide further intuition about the applicability of these methods. We conclude with a simulation study which confirms our findings and show that k-means algorithm, unlike k-principal-components, has serious problems in the setting where many pairs in the groups of concomitant extremes exhibit weak asymptotic dependence. Arguably, this is one of the most important settings from the applications point of view [Davison et al., 2013]. In many other cases the results are almost identical including the 68-dimensional dataset of river discharges analysed at the end.

2. Preliminaries on multivariate extremes

2.1. The angular distribution. Here we recall some elementary theory of multivariate extremes needed in this paper, and refer the reader to the monograph [Resnick, 2008] and surveys [Davison and Huser, 2015, Engelke and Ivanovs, 2020] for further reading. It is a common practice in extremes to first standardize the marginals and then study extremal dependence. Thus we assume that a random vector $Y \in \mathbb{R}^d$, $d \ge 2$, of interest has unit Fréchet marginal distributions: $\operatorname{pr}(Y_i \le y) = \exp(-1/y)$ for y > 0. The fundamental regularity assumption on Y, called multivariate regular variation, can be stated as the

weak convergence of the normalized Y conditional on the norm being large:

$$\frac{Y}{\|Y\|_2} \|Y\|_2 > t \quad \Rightarrow \quad X, \qquad t \to \infty, \tag{1}$$

where the distribution of X is called angular or spectral. This is our main object of interest as it characterizes extremal dependence. It must be noted that any norm can be used here, but we choose the Euclidean norm $\|\cdot\|_2$ so that the angle X lies in the Euclidean simplex $\mathbb{S}^{d-1}_+ = \{x \in \mathbb{R}^d_+ : \|x\|_2 = 1\}$ which is convenient when considering angular dissimilarities in Section 3. Due to marginal standardization, the mean of X must point to the centre of the simplex:

$$E(X_1) = \dots = E(X_d) = \mu > 0.$$
 (2)

This property has a certain balancing effect which will come in use in the following.

The random vector Y satisfying (1) and having unit Fréchet marginals is in the maxdomain of attraction of a max-stable distribution uniquely specified by the angle X. It is said that Y admits asymptotic independence (complete dependence) if the limiting max-stable vector has mutually independent (completely dependent) components. The distribution of the corresponding angle X is then as follows:

- (i) Asymptotic independence: the distribution of X has mass 1/d at every standard basis vector.
- (ii) Asymptotic complete dependence: deterministic $X = (1, ..., 1)/\sqrt{d}$.

A common measure of pairwise asymptotic dependence is the tail dependence coefficient:

$$\chi_{ij} = \lim_{t \to \infty} \operatorname{pr}(Y_j > t \mid Y_i > t) = \frac{1}{\mu} E(X_i \wedge X_j) \in [0, 1],$$

where 0 corresponds to the asymptotic independence in (i) and 1 to the complete dependence in (ii). These are the boundary cases also in other senses as demonstrated by the following simple result.

Lemma 2.1. The constant μ in (2) satisfies $1/d \le \mu \le 1/\sqrt{d}$, where the lower bound is achieved iff case (i) holds, and the upper bound is achieved iff case (ii) holds.

Proof. Note that $\sum_i X_i \ge ||X||_2 = 1$ and take expectation to get the lower bound. The upper bound follows from $1 = \sum_i E(X_i^2) \ge d\mu^2$. Equality in the latter readily implies that all X_i are constant, whereas in the former that $X_i X_j = 0$ a.s. for all $i \ne j$.

In applications it is common to standardize the observations using the empirical marginal distribution functions and then choose threshold t large, but such that sufficiently many approximate angles are obtained for the statistical analysis of extremal dependence. This is exactly the procedure used by [Janssen and Wan, 2020] whose consistency results we will employ in the following. The only difference is that we use unit Fréchet marginals instead of standard Pareto, but these are tail equivalent and no changes in the theory arise.

2.2. Concomitant extremes. In high-dimensional setting it is of crucial importance to identify the non-empty sets of indices $I \subset \{1, \ldots, d\}$ such that $\operatorname{pr}(X_i > 0 \ \forall i \in I, X_j = 0 \ \forall j \notin I) > 0$, and the respective probabilities. We will focus on the maximal sets – those not included in other such sets. Let us define the corresponding faces of \mathbb{R}^d_+ :

$$F_I = \{ x \in \mathbb{R}^d_+ : x_i = 0 \ \forall j \notin I \}. \tag{3}$$

According to (2) the probabilities $pr(X_i > 0)$ are positive for every i, and so every index must be contained in at least one maximal set. The problem at hand is sparse if the cardinality of such sets I is much smaller than d and their number is manageable.

The case (i) of asymptotic independence corresponds to d faces of dimension 1. A more interesting situation occurs when the indices can be partitioned so that asymptotic independence is present between the groups, but not necessarily within these groups. This very basic scenario can be formalized as follows.

Assumption A. There exists $2 \le k \le d$ and a partition (I_1, \ldots, I_k) of the index set $\{1, \ldots, d\}$ such that the respective faces F_{I_1}, \ldots, F_{I_k} form the support of the angular measure: $\operatorname{pr}(X \in F_{I_1} \cup \cdots \cup F_{I_k}) = 1$. Without loss of generality we suppose that the indices in I_u are smaller than those in I_v for all $1 \le u < v \le k$.

Observe that the corresponding faces F_{I_1},\ldots,F_{I_k} are mutually perpendicular: $u^{\scriptscriptstyle \sf T} v=0$ for all $u\in F_{I_i},v\in F_{I_j}$ and $i\neq j$, and the only common element is the origin. Even in this scenario identification of the groups of concomitant extremes I_1,\ldots,I_k using approximate angles may not be straightforward. For a low-dimensional case of d=3 and the partition $I_1=\{1,2\},I_2=\{3\}$ Figure 1 depicts a sample from the exact angular law and two samples from its approximations as could arise in practice for different threshold levels t. We regard this somewhat simplistic scenario of mutually perpendicular faces as a starting point in the analysis of various approaches to identification of concomitant extremes.

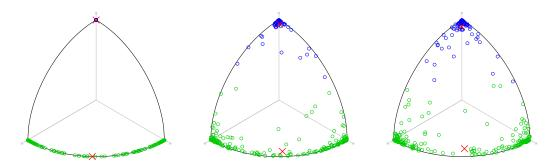


FIGURE 1. A sample of 300 points in \mathbb{S}^2_+ from the exact angular distribution supported by $F_{\{1,2\}} \cup F_{\{3\}}$ and from its approximations. The colors correspond to the spherical 2-means procedure with red crosses being the centroids.

Let us define the corresponding submodels X_I for $I = I_1, \ldots, I_k$ which have the law of the restriction of X to the indices in I conditional on $\{X \in F_I\}$, and let $p_I = \operatorname{pr}(X \in F_I) > 0$ be the respective probabilities. Under Assumption A we thus obtain a complete description of the law of X as a mixture model. Furthermore, $X_I \in \mathbb{S}^{|I|-1}_+$ satisfies (2) with $\mu_I = \mu/p_I$ and so it is a legitimate angular model in dimension |I|. Finally, we define the cross-moment matrices

$$\Sigma_I = E(X_I X_I^{\mathsf{T}}), \qquad \Sigma = E(X X^{\mathsf{T}}) = \operatorname{diag}(p_{I_1} \Sigma_{I_1}, \dots, p_{I_k} \Sigma_{I_k}), \tag{4}$$

where the latter is a block diagonal matrix with $p_I \Sigma_I$ on the diagonal. Note that every Σ_I is a non-negative definite matrix with trace 1, since $||X_I||_2 = 1$. The matrix Σ has been used in extremes before, see Remark 3.3 below.

3. Spherical clustering

3.1. Dissimilarity functions on the simplex and Voronoi diagrams. In this section we consider an arbitrary random variable $X \in \mathbb{S}^{d-1}_+$ not necessarily satisfying (2). Spherical clustering for a given integer $k \geq 1$ amounts to the following stochastic program:

$$\min_{x_1, \dots, x_k \in \mathbb{S}_+^{d-1}} E\left(\min_{i=1}^k c(x_i, X)\right) = 1 - \max_{x_1, \dots, x_k \in \mathbb{S}_+^{d-1}} E\left(\max_{i=1}^k r(x_i^{\mathsf{T}} X)\right), \tag{5}$$

where $c: \mathbb{S}^{d-1}_+ \times \mathbb{S}^{d-1}_+ \mapsto [0,1]$ is a continuous dissimilarity (cost) function. Here we assume that the dissimilarity function has the form $c(x,y) = 1 - r(x^{\mathsf{T}}y)$ for a strictly increasing continuous (reward) function $r:[0,1] \mapsto [0,1]$. In words, the aim is to find k centroids x_i in the simplex such that the expected dissimilarity of X and the closest centroid is minimal. It is noted that the objective function is continuous in (x_1,\ldots,x_k) and the set \mathbb{S}^{d-1}_+ is compact, which readily implies that the minimum must be attained. Uniqueness up to a permutation, however, is not guaranteed.

There is a wide choice of popular angular dissimilarity functions used in a variety of contexts [Palarea-Albaladejo et al., 2012], but the above form has an appealing property

$$c(x_1, y) \le c(x_2, y)$$
 \iff $x_1^{\mathsf{T}} y \ge x_2^{\mathsf{T}} y$ \iff $\|x_1 - y\|_2 \le \|x_2 - y\|_2$

where $x_1, x_2, y \in \mathbb{S}^{d-1}_+$. Thus for the given k points $x_1, \ldots, x_k \in \mathbb{S}^{d-1}_+$ the simplex will be partitioned into clusters A_i by means of hyperplanes in \mathbb{R}^d passing through the origin:

$$A_{i} = \{ y \in \mathbb{S}_{+}^{d-1} : x_{i}^{\mathsf{T}} y \ge x_{i}^{\mathsf{T}} y \ \forall j > i, \ x_{i}^{\mathsf{T}} y > x_{i}^{\mathsf{T}} y \ \forall j < i \}.$$
 (6)

For concreteness, here the equality is broken in favour of the smallest index. Note also that these form the Voronoi diagram of the positive simplex with respect to the Euclidean norm.

The most popular examples of such cost functions are the scaled Euclidean distance, the angular distance and cosine dissimilarity c_1 , plus we additionally define c_2 corresponding to the quadratic reward function $r(u) = u^2$:

$$\sqrt{1-x^{\mathsf{T}}y}$$
, $\langle (x,y) = \frac{2}{\pi}\arccos(x^{\mathsf{T}}y)$, $c_p(x,y) = 1 - (x^{\mathsf{T}}y)^p$, $p = 1, 2$. (7)

The angular distance yields the angle between x and y as the fraction of the right angle $\pi/2$, and such a distance will be useful in numerical experiments below. In clustering one of the most important properties is the simplicity and interpretability of the resulting procedure, and thus we will focus our attention on c_p with p=1,2. In this case the above clustering problem (5) reduces to maximizing the expected maximal reward $(x_i^{\mathsf{T}}X)^p$. For p=1 we retrieve the spherical k-means clustering [Dhillon and Modha, 2001], which is intimately related to the classical k-means. Finally, p=2 leads to, what we call, spherical k-principal-component clustering which is described and analysed below. Even though the literature on clustering is extensive, we could not locate such an approach therein.

3.2. The optimal centroids and partitions. Let us provide some basic results underlying the spherical clustering procedure for the linear and quadratic reward functions. In the first case we will need the normalized means of X restricted to the sets A_i :

$$\overline{x}_i = E(X1_{\{X \in A_i\}}) / \|E(X1_{\{X \in A_i\}})\|_2 \in \mathbb{S}_+^{d-1}, \tag{8}$$

where the partition (A_1, \ldots, A_k) is given by (6) for an arbitrary choice of $x_1, \ldots, x_k \in \mathbb{S}^{d-1}_+$. In order to avoid division by 0 we take $\overline{x}_i = x_i$ when $\operatorname{pr}(X \in A_i) = 0$. In the second case we define $d \times d$ matrices

$$\Sigma_i = E(XX^{\mathsf{T}} \mathbf{1}_{\{X \in A_i\}}), \qquad i = 1, \dots, k. \tag{9}$$

Note the difference between Σ_i and $\Sigma_{\{i\}}$ defined in Section 2. These are non-negative symmetric matrices, which are also non-negative definite. We will be interested in the largest eigenvalue $\lambda_1(\Sigma_i)$ and the corresponding eigenvector \hat{x}_i of Σ_i , assumed to have unit norm: $\|\hat{x}_i\|_2 = 1$. There may be more than one such eigenvector, but at least one of them must have non-negative entries by the Perron–Frobenius theorem, and we choose such. Hence we may assume that $\hat{x}_i \in \mathbb{S}^{d-1}_+$. If the matrix Σ_i is positive or at least irreducible then such a vector is unique.

The first result forms the basis of the clustering procedure, see [Dhillon and Modha, 2001, Lem. 3.1] for the sample version in the case of the spherical k-means algorithm.

Proposition 3.1. For $x_1, \ldots, x_k \in \mathbb{S}^{d-1}_+$ consider the partition (A_i) in (6). Then

$$E\left(\max_{i=1}^k x_i^{\mathsf{T}} X\right) \le E\left(\max_{i=1}^k \overline{x}_i^{\mathsf{T}} X\right), \qquad E\left(\max_{i=1}^k (x_i^{\mathsf{T}} X)^2\right) \le E\left(\max_{i=1}^k (\hat{x}_i^{\mathsf{T}} X)^2\right),$$

where \overline{x}_i are the normalized means defined in (8) and \hat{x}_i are the normalized principal eigenvectors of matrices Σ_i defined in (9).

Proof. By definition of A_i and \overline{x}_i we readily obtain

$$E\left(\max_{i=1}^k x_i^{\mathsf{T}} X\right) = \sum_{i=1}^k x_i^{\mathsf{T}} E(X \mathbf{1}_{\{X \in A_i\}}) \le \sum_{i=1}^k \overline{x}_i^{\mathsf{T}} E(X \mathbf{1}_{\{X \in A_i\}}) \le E\left(\max_{i=1}^k \overline{x}_i^{\mathsf{T}} X\right),$$

where the last inequality follows from the fact that only one term among $X1_{\{X\in A_i\}}$ is non-zero.

By definition of Σ_i we have

$$E\left(\max_{i=1}^{k} (x_i^{\mathsf{T}} X)^2\right) = \sum_{i=1}^{k} E(x_i^{\mathsf{T}} X \mathbf{1}_{\{X \in A_i\}})^2 = \sum_{i=1}^{k} x_i^{\mathsf{T}} \Sigma_i x \le \sum_{i=1}^{k} \hat{x}_i^{\mathsf{T}} \Sigma_i \hat{x}_i = \sum_{i=1}^{k} \lambda_1(\Sigma_i), \tag{10}$$

where we use the standard fact that the quadratic form is maximized under the constraint $||x||_2 = 1$ by the principal eigenvector and the maximal value is given by the corresponding eigenvalue, see, e.g., [Overton and Womersley, 1992, Thm. 1]. It is left to observe that

$$\sum_{i=1}^{k} \hat{x}_{i}^{\mathsf{T}} \Sigma_{i} \hat{x}_{i} = \sum_{i=1}^{k} E(\hat{x}_{i}^{\mathsf{T}} X \mathbf{1}_{\{X \in A_{i}\}})^{2} \le E\left(\max_{i=1}^{k} (\hat{x}_{i}^{\mathsf{T}} X)^{2}\right),\tag{11}$$

since only one term among $X1_{\{X\in A_i\}}$ is non-zero.

The above result suggests an iterative procedure for finding the optimal centroids where the updates \overline{x}_i , respectively \hat{x}_i , of the current centroids x_i are used. This procedure will normally converge to a local maximum for the linear, respectively quadratic, reward function. By using a number of different starting centroids we may hope to discover the global maximum and thus solve (5) for the dissimilarity functions c_1 and c_2 . This is exactly the spherical k-means procedure when c_1 and hence the means \overline{x}_i are used.

Importantly, instead of centroids we may optimize over partitions of the simplex.

Corollary 3.2 (Duality). Let \mathcal{P}_k be the set of partitions of \mathbb{S}^{d-1}_+ into k Borel sets. Then

$$\max_{x_1, \dots, x_k \in \mathbb{S}_+^{d-1}} E\left(\max_{i=1}^k x_i^{\mathsf{T}} X\right) = \max_{(A_1, \dots A_k) \in \mathcal{P}_k} \sum_{i=1}^k \|E(X \mathbf{1}_{\{X \in A_i\}}\|_2,$$

$$\max_{x_1,\dots,x_k\in\mathbb{S}_+^{d-1}} E\left(\max_{i=1}^k (x_i^\intercal X)^2\right) = \max_{(A_1,\dots A_k)\in\mathcal{P}_k} \sum_{i=1}^k \lambda_1(\Sigma_i),$$

where Σ_i are defined in (9). Moreover,

- every optimizer (x_1, \ldots, x_k) yields an optimal partition (A_1, \ldots, A_k) via (6);
- every optimal partition $(A_1, ..., A_k)$ yields an optimal $(x_1, ..., x_k)$ given by $x_i = \overline{x_i}$ in the first case and $x_i = \hat{x_i}$ in the second.

Proof. The proof of the two cases is analogous, and we consider the second case only. Let $x_1, \ldots, x_k \in \mathbb{S}_+^{d-1}$ be an optimal solution to the left hand side problem, which exists. By the maximality and (10) we find that the optimal value is $\sum_{i=1}^k \hat{x}_i^{\mathsf{T}} \sum_i \hat{x}_i = \sum_{i=1}^k \lambda_1(\Sigma_i)$. Thus the supremum over partitions is no smaller. Take an arbitrary partition $(A_1, \ldots, A_k) \in \mathcal{P}_k$ with the respective \hat{x}_i and observe that the associated value cannot exceed the maximum over the centroids, see (11). Hence the supremum over the partitions is achieved and the optimal values coincide.

Remark 3.3. Matrices Σ_i , up to the restriction $X \in A_i$, are the matrices used by [Cooley and Thibaud, 2019] and [Drees and Sabourin, 2019] in their principal component analysis of extremal dependence. In this respect, we note that finding the best direction for $X \in \mathbb{S}^{d-1}_+$ corresponds to minimizing the expected c_2 dissimilarity:

$$\min_{x:\|x\|_2=1} E\left(\|X-(x^{\mathsf{T}}X)x\|_2^2\right) = 1 - \max_{x:\|x\|_2=1} E(x^{\mathsf{T}}X)^2 = \min_{x:\|x\|_2=1} E\left(c_2(x,X)\right).$$

This provides a link between our clustering approach and principal component analysis for a distribution on a positive simplex.

3.3. Spherical k-principal-components algorithm. Here we state the algorithm for a discrete distribution putting mass 1/n at points $\theta_1, \ldots, \theta_n \in \mathbb{S}^{d-1}_+$, not necessarily distinct. Clearly, this setting includes the empirical law. Only a single iteration is described, since the rest is standard.

Algorithm 1: Spherical k-principal-components clustering – a single iteration.

Input: the sample $\theta_1, \dots, \theta_n \in \mathbb{S}^{d-1}_+$ and current centroids $x_1, \dots, x_k \in \mathbb{S}^{d-1}_+$.

Compute $n \times k$ matrix of dot products $M = (\theta_1, \dots, \theta_n)^{\mathsf{T}}(x_1, \dots, x_k)$

Let v be the mean of row-wise maxima of M

For each row of M find the index of the (first) maximal value and store them in g For i = 1 to i = k

Calculate $\Sigma_i = \frac{1}{n} \sum_{u=1}^n (\theta_u \theta_u^{\mathsf{T}} \mathbf{1}_{\{g_u = i\}})$

Find the principal eigenvector $\hat{x}_i \in \mathbb{S}^{d-1}_+$ of Σ_i

Output: new centroids $\hat{x}_1, \dots, \hat{x}_k \in \mathbb{S}^{d-1}_+$ and the old value v.

It is easy to see that the running time complexity of this algorithm is O(k(nd+f(d))), where f(d) is the complexity of finding the principal eigenvector of $d \times d$ non-negative symmetric matrix, see [Wang et al., 2018] for some basic algorithms and recent developments in this field. Assuming that the spectral gap is bounded away from 0 we may take $f(d) = d^2 \log d$, making both clustering algorithms comparable in the common situation when $d \log d \le n$.

4. Clustering in identification of concomitant extremes

4.1. **Problem formulation.** The main goal of this work is to provide some theoretical results supporting clustering for identification of concomitant extremes. The dissimilarities c_1 and c_2 are continuous and hence the consistency result [Janssen and Wan, 2020, Prop. 3.3] readily applies to both types of spherical clustering described above. In words, for high enough threshold t yielding sufficiently many large observations we may expect that clustering of the approximate angles will result in centroids x_1, \ldots, x_k close to the true centroids of the angular distribution, given the latter ones are unique up to a permutation. Thus we may focus on clustering of the exact angular distribution, that is, the distribution of X. The balancing condition (2) will play a crucial role on this way. Some results are still true without this condition and so we stress when it is indeed required.

The very basic scenario is stated in Assumption A, and it gives rise to the fundamental question concerning applicability of clustering to concomitant extremes:

Will clustering of X under Assumption A produce one centroid in each face?

We will see that this is not always the case, and our goal is to identify simple interpretable conditions implying such a result. It turns out that spherical k-principal-components is preferable to spherical k-means in this setting, since it is more robust and also allows for a substantial theory.

Figure 1 illustrates the spherical k-means clustering in the simple case of d=3 and different approximation levels of the angular distribution. The spherical k-principal components clustering results in exactly the same assignment of all points (blue/green) to the clusters. The centroids for the two methods are close to each other and also close to the respective faces, and in the case of sampling from the exact law they are, in fact, on the faces $F_{\{1,2\}}$ and $F_{\{3\}}$.

4.2. Fundamental observations. Our analysis will rely on the following characterization result, which readily follows from the clustering duality in Corollary 3.2. Recall the definition of the submodels X_I in Section 2 and that \mathcal{P}_k is the set of all partitions of \mathbb{S}^{d-1}_+ into k Borel sets (or sets of the form (6)).

Proposition 4.1. Under Assumption A the following is true.

• k-means: There exist optimal centroids $x_1 \in F_{I_1}, \dots, x_k \in F_{I_k}$ iff

$$\sum_{I=I_1,\dots,I_k} p_I \| E(X_I) \|_2 = \max_{(A_1,\dots,A_k) \in \mathcal{P}_k} \sum_{i=1}^k \| E(X \mathbf{1}_{\{X \in A_i\}}) \|_2, \tag{12}$$

where the left hand side is $\mu(\sqrt{|I_1|} + \cdots + \sqrt{|I_k|})$ assuming (2).

• k-principal-components: There exist optimal centroids $x_1 \in F_{I_1}, \ldots, x_k \in F_{I_k}$ iff

$$\sum_{I=I_1, \dots, I_k} p_I \lambda_1(\Sigma_I) = \max_{(A_1, \dots, A_k) \in \mathcal{P}_k} \sum_{i=1}^k \lambda_1 \left(E(XX^{\mathsf{T}} \mathbf{1}_{\{X \in A_i\}}) \right). \tag{13}$$

Proof. We focus on the k-means since the other result is analogous. Note that the left hand side of (12) is just $\sum_{i=1}^{k} \|E(X1_{\{X \in F_{I_i}\}})\|_2$ and so by Corollary 3.2

$$x_i = E(X1_{\{X \in F_{I_i}\}}) / \|E(X1_{\{X \in F_{I_i}\}})\|_2$$

yields an optimal set of centroids, since the given disjoint sets $F_{I_u} \cap \mathbb{S}^{d-1}_+$ can be extended to a partition of \mathbb{S}^{d-1}_+ . These indeed satisfy $x_i \in F_{I_i}$.

Next, suppose that some $x_i \in F_{I_i}$ are optimal, and let A_i be the sets in (6), which then yield the maximum. The faces are mutually orthogonal and so every vector $y \in A_i$ in the support of X also belongs to F_{I_i} , unless $x_i^{\mathsf{T}}y = 0$ for all i. The latter vectors can be reshuffled between the associated clusters without changing the cost. So we may restrict A_i to F_{I_i} and the first statement follows. Moreover, assuming (2) we have $E(X_I) = \mu_I(1, \ldots, 1)^{\mathsf{T}}$ and so its norm is $\mu_I \sqrt{|I|}$.

In the case of k-principal-components we also need to observe that the principal eigenvector of $E(XX^{\mathsf{T}}1_{\{X\in F_{I_i}\}})$ indeed belongs to F_{I_i} , and the corresponding eigenvalue is $p_{I_i}\lambda_1(\Sigma_{I_i})>0$.

A simple critical test of any approach is given by the angular distribution corresponding to the asymptotic independence, see case (i) in Section 2. In this case any partition of indices yields faces satisfying Assumption A. We take k=2 for simplicity and partition the index set into $I_1 = \{1, \ldots, d_1\}$ and $I_2 = \{d_1 + 1, \ldots, d\}$ for some $1 \le d_1 \le d - 1$.

For k-means the necessary and sufficient condition (12) reads

$$\sqrt{d_1} + \sqrt{d - d_1} = \max_{\ell = 0, \dots, d} \{ \sqrt{\ell} + \sqrt{d - \ell} \},$$

where ℓ and $d - \ell$ correspond to the alternative partition. But the right hand side is maximized at $\ell = d/2$ when d is even and $\ell = (d\pm 1)/2$ when d is odd, and so we must choose index sets of essentially equal size to make clustering 'work', see also Proposition 4.2 below. In the k-principal-components case we note that $\lambda_1(E(XX^{\mathsf{T}}1_{\{X\in A_i\}})) = 1/d$ whenever A_i contains at least one standard basis vector. Thus the necessary and sufficient condition (13) always holds for such X.

In the above case the partitioning is arbitrary, but one can always construct another angle X' satisfying the moment constraints and arbitrarily close to X such that a given partition becomes the only correct one (the respective faces support the law of X'). This provides a class of examples where k-means clustering fails to identify the supporting faces, because the dissimilarity is continuous. Importantly, k-principal-components does not readily fail in this case.

4.3. Spherical k-means in the size-balanced case. For the spherical k-means procedure we only have a result when the dimensions of the faces satisfy a certain strict condition. If this assumption is violated, it is possible to construct a model where k-means fails to identify the correct faces. It is sufficient to have an alternative partition into faces with a larger value of $\sqrt{|I_1|} + \cdots + \sqrt{|I_k|}$, or rather a model relatively close to that. This observation readily follows from Proposition 4.1.

Proposition 4.2. Suppose Assumption A and (2) hold. If $d_1 = |I_1|, \ldots, d_k = |I_k|$ yield the maximum in

$$\max_{\substack{d_1,\dots,d_k\in\mathbb{N}_0\\d_1+\dots+d_k=d}} \sqrt{d_1} + \dots \sqrt{d_k},$$

then there exist optimal centroids (x_1, \ldots, x_k) of the spherical k-means clustering with $x_i \in F_{I_i}$ for all i. For k = 2 this condition reads $||I_1| - |I_2|| \le 1$.

Proof. In view of (12) it is only required to show that

$$\mu(\sqrt{d_1} + \dots + \sqrt{d_k}) \ge \sum_{i=1}^k ||E(X1_{\{X \in A_i\}})||_2$$

for any partition $(A_1, \ldots, A_k) \in \mathcal{P}_k$. We denote the right hand side by $\sum_{i=1}^k \|\nu_i\|_2$ and note that its maximum over $\nu_i \in \mathbb{R}^d_+$ subject to the constraint $\sum \nu_i = E(X) = \mu(1, \ldots, 1)^{\mathsf{T}}$ is attained under the assumption $\nu_i \perp \nu_j$ for all $i \neq j$, see Lemma A.1. Letting δ_i be the number of non-zero entries in ν_i we get an upper bound on the sum of norms:

$$\mu(\sqrt{\delta_1} + \dots + \sqrt{\delta_k})$$

and the first statement follows. The case k=2 has been discussed above and here the optimal integers d_1, d_2 are such that $|d_1 - d_2| \le 1$, and the proof is complete.

5. Spherical k-principal-components clustering

5.1. The main result. The eigenvalues of the matrices Σ_I corresponding to the submodels, see Section 2, will play a crucial role in the following. When discussing some basic properties of these matrices we write Σ and assume that $d \geq 1$. Also, let $\lambda_j(M)$ denote the jth largest eigenvalue of a symmetric matrix M, tacitly assuming $\lambda_j(M) = 0$ when j exceeds the order of M. In the case (i) of asymptotic independence Σ is a diagonal matrix with 1/d on the diagonal, so that $\lambda_1(\Sigma) = \lambda_2(\Sigma) = 1/d = \mu$. In the case (ii) of complete dependence Σ is a matrix with constant elements 1/d yielding $\lambda_1(\Sigma) = 1, \lambda_2(\Sigma) = 0$. The following lower bound on the largest eigenvalue is true in general.

Lemma 5.1. Consider $\Sigma = E(XX^{\mathsf{T}})$, where $X \in \mathbb{S}^{d-1}_+$ with $d \geq 1$ satisfies (2). Then

$$\lambda_1(\Sigma) \geq \mu$$
,

and the equality implies asymptotic independence.

Proof. Consider the decomposition $\Sigma = \Sigma_0 + \mu^2 \mathbf{1} \mathbf{1}^{\mathsf{T}}$, where Σ_0 is the respective covariance matrix and $\mathbf{1}$ is a vector of ones. All three matrices are non-negative definite, and the eigenvalues of the latter are $d\mu^2, 0, \ldots, 0$. Next, we use the standard inequality: $\lambda_1(\Sigma) \geq \lambda_1(\mu^2 \mathbf{1} \mathbf{1}^{\mathsf{T}}) = d\mu^2$, which follows from the interpretation of λ_1 as the maximum over quadratic forms, for example. Apply Lemma 2.1 to conclude.

We are now ready to state our main result providing some basic theory supporting the use of clustering in detection of groups of concomitant extremes.

Theorem 5.2. Suppose Assumption A holds. If

$$\min_{I=I_1,\dots,I_k} p_I \lambda_1(\Sigma_I) \ge \max_{I=I_1,\dots,I_k} p_I \lambda_2(\Sigma_I), \tag{14}$$

then there exist optimal centroids $(x_1, ..., x_k)$ of the spherical k-principal-components clustering such that $x_i \in F_{I_i}$ for all i. Moreover, this condition is satisfied when (2) holds and

$$\lambda_2(\Sigma_I) \le \mu_I \qquad I = I_1, \dots, I_k. \tag{15}$$

Importantly, this sufficient condition asserts that the second principal direction for any face provides a smaller loss reduction than the principal direction of any other face taking the respective probability weights into account. That is, the problem is balanced in this sense. Moreover, the above condition is implied when μ_I separates the first two eigenvalues of Σ_I for all submodels I, see Lemma 5.1. This is true, for example, for certain symmetric models, see Lemma 5.4 below, irrespective of the dimension.

of Theorem 5.2. Let $D_i = p_{I_i} \Sigma_{I_i}$ be the diagonal blocks of Σ . In view of (13) it is only required to show for any partition $(A_1, \ldots, A_k) \in \mathcal{P}_k$ that

$$\sum_{i=1}^{k} \lambda_1(D_i) \ge \sum_{i=1}^{k} \lambda_1(\Sigma_i),$$

where $\Sigma_i = E(XX^{\mathsf{T}}1_{\{X\in A_i\}})$. Lemma A.2 in Appendix A is crucial here, and it shows that the right hand side is upper bounded by $\sum_{i=1}^k \lambda_i(\Sigma)$. Thus it is left to show that $\sum_{i=1}^k \lambda_1(D_i) \geq \sum_{i=1}^k \lambda_i(\Sigma)$, which is indeed equivalent to the stated assumption, because of the block diagonal structure of $\Sigma = \operatorname{diag}(D_1, \ldots, D_k)$.

Now suppose that (2) and (15) are in place. Then

$$\max_{I} \{ p_{I} \lambda_{2}(\Sigma_{I}) \} \leq \mu \leq \min_{I} \{ p_{I} \lambda_{1}(\Sigma_{I}) \},$$

where we apply Lemma 5.1 to each Σ_I .

5.2. Simple sufficient conditions. Let us discuss the condition in (15) for a fixed I. Firstly, it is always true for a one or two-dimensional face, where in the former case we tacitly assume that $\lambda_2 = 0$.

Lemma 5.3. Assume (2) and d = 2. Then $\lambda_2(\Sigma) \leq \mu$.

Proof. We have $\lambda_1 + \lambda_2 = \text{tr}\Sigma = 1$, and $\lambda_1 \ge \mu$ by Lemma A.2. By Lemma 2.1, $\mu \ge 1/2$, and so

$$\lambda_2 = 1 - \lambda_1 \le 1 - \mu \le \mu,$$

which completes the proof.

Secondly, certain symmetries imply this condition as, for example, invariance of the second moments under permutation.

Lemma 5.4. Assume (2) and $E(X_iX_j) = E(X_{\pi(i)}X_{\pi(j)})$ for all i, j and all permutations π . Then $\lambda_2(\Sigma) \leq 1/d \leq \mu$.

Proof. Let $c = E(X_1X_2) \ge 0$ be the common cross-moment. Observe from $||X||_2 = 1$ that $EX_1^2 = 1/d$, so that Σ is a matrix with diagonal elements 1/d and off-diagonal c. It is not difficult to check that $\lambda_1 = 1/d + (d-1)c$ and the other eigenvalues are all equal to 1/d - c. The proof is complete in view of Lemma 2.1.

5.3. Counterexamples. A basic counterexample is obtained by considering more groups of (almost) concomitant extremes than there are clusters. Assume that the index set can be partitioned into 3 sets I_1, I_2, I_3 , but we use k = 2 with the partition I_1 and $I_2 \cup I_3$. Write $\Sigma = \text{diag}(D_1, D_2, D_3)$ and suppose that the leading eigenvalues satisfy

$$\lambda_1(D_1) < \lambda_1(D_2) \le \lambda_1(D_3).$$

This, for example, occurs when $|I_1| = 1$ and $|I_2|, |I_3| > 1$ with the latter two submodels being asymptotically dependent. Now $\lambda_1(D_1) = \mu$ and the others are larger according to Lemma 5.1. Other examples with $|I_1| > 1$ can be obtained by imposing higher dependence in the faces joined into a single group. Then not only the sufficient condition (14) fails, but also the result is no longer true, since an alternative partition $I_1 \cup I_2$ and I_3 produces a strictly larger value:

$$\lambda_1(D_2) + \lambda_1(D_3) > \lambda_1(D_1) + \lambda_1(D_3).$$

It is thus left to apply Proposition 4.1 to see that the k-principal components clustering fails to determine the assumed groups. Of course, the failure is due to the wrong grouping of the three faces, but by continuity of the dissimilarity function we can perturb the model by introducing some small mass on $F_{I_2 \cup I_3}$ without drastically changing the location of the optimal centroids, but making the partition I_1 and $I_2 \cup I_3$ the only possibility.

6. Numerical experiments

6.1. The simulation framework. We take k = 2 faces in d = 100 dimensional setting. The dimensions d_1 and $d_2 = d - d_1$ of the submodels will be chosen later. The random vector Y is taken to have a d-variate max-stable Hüsler–Reiss distribution introduced in [Hüsler and Reiss, 1989] and further studied in [Engelke et al., 2015, Engelke and Hitz, 2020]. This popular family has a good control of pairwise extremal dependencies which are encoded into the associated variogram matrix Γ parametrising the distribution. The variogram ensuring Assumption A is produced randomly in a certain way detailed in Appendix B, where we also show that Σ has a simple expression in terms of the expectations of the transformed (d-1)-dimensional normal vectors derived from the matrix Γ in a standard way [Engelke et al., 2015]. The exact Σ is not required for our simulations.

Detecting the faces would be a simple task if asymptotic dependence within each face was high. Thus we ensure that the pairwise tail dependence coefficients are likely to be very small in our parameter generation procedure: χ_{ij} has mean 0.2, and it is below 0.1 with probability 0.23 for every pair $i \neq j$ in the same group. This may lead to a subdivision of a group of concomitant extremes into almost independent subgroups making the detection problem much harder, see Section 4. Note that χ_{ij} has an explicit expression in terms of Γ_{ij} and need not be estimated from approximate angles.

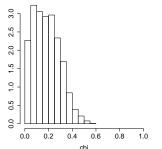
In each experiment we sample 10^4 iid realizations of Y using the R package [Engelke et al., 2019]. We take 10% of these vectors having the largest Euclidean norm and thus form 10^3 approximate realizations of the angle X.

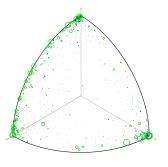
One way to obtain faces from either the approximate angles or the centroids $x \in \mathbb{S}^{d-1}_+$ is to use a simple truncation procedure: $I = \{i : x_i > \epsilon\}$ for a chosen level $\epsilon > 0$. Another way is to find the index set I with the minimal cardinality and such that the angle with the respective face is sufficiently small $\langle (x, F_I) \rangle \langle \epsilon$, where

$$\langle (x, F_I) = \min\{\langle (x, y) : y \in F_I \cap \mathbb{S}^{d-1}_+\} = \frac{2}{\pi} \arccos\left[\left(\sum_{i \in I} x_i^2\right)^{1/2}\right], \tag{16}$$

see also (7). The last equality follows from the fact that the minimizer y is given by the normalized vector $(x_i 1_{\{i \in I\}})_{i=1}^d$. Finding such I is thus simple, since we only need to choose enough indices corresponding to the largest x_i 's. Note that by doing so we always pick a face yielding the smallest angle with x among all faces of the same dimension. This latter approach is more consistent with the spherical clustering paradigm and it produces somewhat more stable results in our experiments. In fact, any dissimilarity in Section 3 would produce the same results up to changing the threshold appropriately.

6.2. Illustration of the detection procedure. In this experiment we take $d_1 = 30$ and $d_2 = 70$. We simulate the variogram Γ and data only once and then illustrate the detection procedure. A histogram of exact χ_{ij} with $i \neq j$ being in the same group is shown in Figure 2, and we note that 27.5% of these are below 0.1 making the data look as being asymptotically independent for the respective pairs.





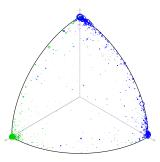
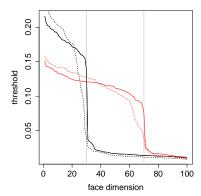


FIGURE 2. A histogram of (χ_{ij}) , angles projected on $F_{\{1,2,3\}}$ and $F_{\{1,31,32\}}$ with k-principal-components clustering in green and blue.

Furthermore, we plot the sampled angles when projected on the faces $F_{\{1,2,3\}}$ and $F_{\{1,31,32\}}$. The scale of the points corresponds to the norms of the projections. Note that the data does exhibit high degree of asymptotic independence and the respective summaries are $\chi_{12} = 0.12$, $\chi_{13} = 0.39$, $\chi_{23} = 0.11$ and $\chi_{1,31} = \chi_{1,32} = 0$, $\chi_{31,32} = 0.23$.

We apply spherical k-means and k-principal-components algorithms using 100 runs for each. Both algorithms do not improve when additional 100 runs are used. Both centroids are close to the respective faces with the angles (16) being 0.15 and 0.1 for k-means and 0.08 and 0.06 for k-principal-components. Thus we may easily associate centroids with the respective faces in this case. The angular difference between the centroids from the different methods is 0.17 and 0.11.



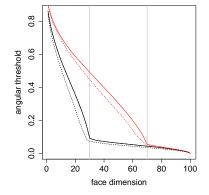
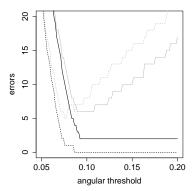


FIGURE 3. The sorted entries of the four centroids (dashed for k-principal-components), and the minimal angles. Grey lines indicate the correct dimensions.

Choosing a threshold to define faces is a hard task in general. Figure 3 depicts the sorted entries of the four centroids, and the angles to the faces identified by the largest entries. These can be interpreted as the smallest angles to any face of the given dimension. Additional smoothness comes from taking sums of the squared largest entries in the angle calculation in (16). Note that both plots indicate a sudden change at dimensions of about 30 and 70 which are denoted by grey vertical lines. It also suggests numbers around 0.03 and 0.1 for the entry-wise and angular thresholds, respectively.

Finally, we apply the two thresholding procedures and report in Figure 4 the number of errors for each method and the threshold used.



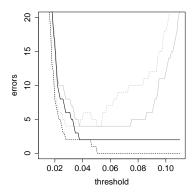
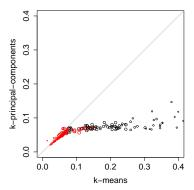


FIGURE 4. The total number of added indices in detection of faces (dashed for k-principal-components) when using entry-wise and angular thresholding. The counts of both added and removed indices are in grey.

More precisely, we count the indices suggested by a centroid which do not belong to its face, and then add up the two numbers for each method. In grey we depict the counts of both the added and removed indices. Our focus is on the added indices, because these lead to the expansion of the face, whereas removal leads to focusing on a subgroup of concomitant extremes. Note, however, that taking an overly large entry-wise threshold may lead to an empty set, and the results for large threshold values should be interpreted with care. In conclusion, both methods are comparable with k-principal-components being slightly better with respect to the added indices.



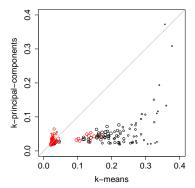


FIGURE 5. (i) angles to the corresponding faces and (ii) maximal entries over I^c with scale corresponding to the dimension of d_1 and colour to the face.

6.3. Comparison of clustering approaches. We replicate our experiment 100 times, each time randomly generating variogram Γ and randomly choosing $d_1 \in \{1, ..., 50\}$. For each method and each centroid x we calculate the angle to the corresponding face $\langle (x, F_I) \rangle$ defined in (16) and the maximal entry $\max\{x_i : i \notin I\}$ over the indices defining the other face. That is, small number indicates that the centroid is indeed very close to its face, see Figure 5 where 19 and 8 black points are outside of plot range, respectively.

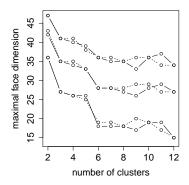
We call it an error when a centroid yields the angle and the maximal entry both exceeding 0.1. Out of 200 trials (faces) there are approximately 46% errors for k-means and only 8% for k-principal components, and all of the latter are also the errors in k-means.

By increasing the threshold to 0.2 we get 26% and 5% of errors, and again all the errors in the latter are also errors in the former. Furthermore, these correspond to the first face and occur when it is relatively small. We also check that in all these cases permuting the assignment to faces does not resolve the issue.

In conclusion, in a weak asymptotic dependence regime the k-principal components method outperforms k-means, which is also expected in view of the above developed theory and accompanying intuition. In the case of increased dependence within the faces both clustering methods perform extremely well making identification of the corresponding faces an obvious task. But even in this simple-looking setting the direct approach based on data thresholding fails to provide any useful information, even upon further aggregation and threshold tuning.

6.4. An application to river discharges. We illustrate the two clustering approaches using river discharges at d=68 locations in Switzerland, see the review paper [Engelke and Ivanovs, 2020] for a detailed description of this dataset. The threshold t in (1) is chosen such that 10% of observations are used to approximate the angular distribution, resulting in 202 samples. Unlike in the simulation experiments above, here we have a rather strong 'asymptotic' dependence between various components, and no underlying partition into faces can be expected.

We consider a relatively small number of clusters k = 2, ..., 12, which is desirable in practice since every cluster leads to a submodel requiring further investigation. It must also be noted that clustering is a computationally hard problem (NP-hard), and the cost function in real world problems is likely to exhibit many more local minima compared to the simulated examples above. Furthermore, larger numbers of clusters normally lead to worse approximations, whereas both clustering approaches are expected to produce rather similar results. In order to limit the effect of suboptimal centroids on the comparison of the methods we (randomly) restart each clustering procedure 30,000 times. Note that a much smaller number of restarts should be sufficient in practice. In all cases the centroids produced by the two methods are very similar with the maximal angular distance of 0.1.



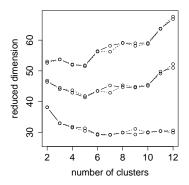
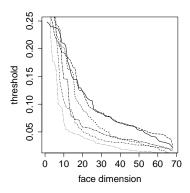


FIGURE 6. Maximal face dimension and total dimension for angular thresholds 1/5, 1/4, 1/3 with dashed lines for k-principal-components.

The standard 'elbow plot' of the cost as a function of k does not reveal a clear candidate for the number of clusters, and so is omitted. Importantly, our final goal is not to cluster the points but rather to determine the groups of concomitant extremes, hopefully leading to a sparse model. Thus instead of plotting the cost function we plot certain statistics of the detected faces using a number of thresholds. The angular threshold results in

better-behaved plots and we chose $\epsilon = 1/5, 1/4, 1/3$ in Figure 6, where the statistics are (a) the maximal face dimension and (b) the reduced dimension. The latter is given by $f^{-1}(\sum_{i=1}^{i=k} f(d_i))$ with f(d) = d(d-1)/2 representing the number of parameters needed in the Hüsler-Reiss model of dimension d. The maximal face dimension in Figure 6 suggests k = 6, whereas the total dimension somewhat prefers k = 5.



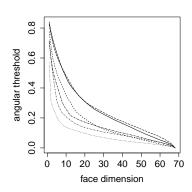


FIGURE 7. Threshold plots for k = 6.

We further analyse the output for k=6, see Figure 7 presenting threshold plots mimicking those in Figure 3. Here we use k-principal-components centroids, but the others are extremely close and result in similar plots. These plots indicate that different centroids may require different thresholds, and this is easy to implement using our angular thresholding approach. The obtained 6 groups of concomitant extremes exhibit nice geographical patterns.

In conclusion, the spherical clustering approach is an indispensable tool in the analysis of concomitant extremes in large dimensions. The two methods often produce similar results, but the k-principal-components method may be much better in the setting when the groups exhibit weak asymptotic dependence between many pairs of their components.

ACKNOWLEDGEMENT

The authors gratefully acknowledge financial support of Sapere Aude Starting Grant 8049-00021B "Distributional Robustness in Assessment of Extreme Risk".

APPENDIX A. TWO LEMMAS

The first result is required for the proof of Proposition 4.2.

Lemma A.1. A maximizer (ν_1, \ldots, ν_k) of

$$\max_{\nu_1,\dots,\nu_k\in\mathbb{R}^d_+}\sum_{i=1}^k\|\nu_i\|_2 \qquad subject\ to \qquad \sum_{i=1}^k\nu_i=\nu\in\mathbb{R}^d_+$$

satisfies for all $i \neq j$: $\nu_i \perp \nu_j$ or both ν_i and ν_j have one positive entry at the same position. Moreover, if $k \leq d$, then the maximum is attained under the assumption $\nu_i \perp \nu_j$ for all $i \neq j$.

Proof. The maximum is attained since it is the maximum of a continuous function over a compact set. Assume that for some index ℓ we have $a = \nu_{i\ell} > 0$ and $b = \nu_{j\ell} > 0$, which is equivalent to $\nu_i \pm \nu_j$. Let $c = (\sum_{m \neq \ell} \nu_{im}^2)^{1/2} \ge 0$ and $d = (\sum_{m \neq \ell} \nu_{jm}^2)^{1/2} \ge 0$ be the norms

when the ℓ th coordinate is ignored. We further assume that c+d>0, which excludes the possibility of only one positive entry. It is enough to show that there exists a vector $u \in \mathbb{R}^d$ such that

$$\|\nu_i + u\|_2 + \|\nu_j - u\|_2 > \|\nu_i\|_2 + \|\nu_i\|_2, \qquad \nu_i + u, \nu_i - u \ge 0,$$

so that the maximality fails. We will consider the two possibilities $u = be_{\ell}$ and $u = -ae_{\ell}$, where e_{ℓ} is the ℓ th standard basis vector. It is clear that the positivity constraint is satisfied. Thus it is enough to show that

$$\max\{\sqrt{(a+b)^2 + c^2} + d, c + \sqrt{(a+b)^2 + d^2}\} > \sqrt{a^2 + c^2} + \sqrt{b^2 + d^2},\tag{17}$$

where a, b > 0, $c, d \ge 0$ and c + d > 0, which can be proved by assuming that d > c so that the first entry in the maximum is larger than the second, and taking squares of both sides twice.

Finally, any group of ν_i with a single strictly positive entry in the same position can be replaced by their sum and zero vectors without changing the sum of norms.

The proof of Theorem 5.2 relies on the following non-standard upper bound on the sum of leading eigenvalues.

Lemma A.2. Let $M_1 \ldots, M_k$ be symmetric non-negative definite matrices of order $d \ge k$. Then

$$\sum_{i=1}^{k} \lambda_1(M_i) \le \sum_{i=1}^{k} \lambda_i(M), \qquad M = \sum_{i=1}^{k} M_i.$$
 (18)

Moreover, for any M there exists M_i as above yielding the equality.

Proof. By the result of [Fan, 1949], see also [Overton and Womersley, 1992, Thm. 1], we have

$$\sum_{i=1}^{k} \lambda_i(M) = \max \left\{ \sum_{i=1}^{k} v_i^{\mathsf{T}} M v_i : v_i^{\mathsf{T}} v_j = 1_{\{i=j\}} \right\}$$
 (19)

and, in particular, $\lambda_1(M) = \max\{v^{\mathsf{T}} M v : ||v||_2 = 1\}.$

Let vectors u_1, \ldots, u_k have unit norms and be such that $\lambda_1(M_i) = u_i^{\mathsf{T}} M_i u_i$, and let v_1, \ldots, v_k be mutually orthogonal vectors with unit norms obtained via the Gram-Schmidt process. That is, for all $i = 1, \ldots, k$ we have $u_i = \sum_{j=1}^i c_{ij} v_j$, where $\sum_{j=1}^i c_{ij}^2 = 1$.

By (19) we have

$$\sum_{j=1}^{k} \lambda_j(M) \ge \sum_{j=1}^{k} v_j^{\mathsf{T}} M v_j = \sum_{i=1}^{k} \sum_{j=1}^{k} v_j^{\mathsf{T}} M_i v_j \ge \sum_{i=1}^{k} \sum_{j=1}^{i} v_j^{\mathsf{T}} M_i v_j,$$

where in the last step we use the assumption that M_i are non-negative definite. Furthermore, for any i we have the representation

$$\lambda_1(M_i) = u_i^{\mathsf{T}} M_i u_i = \left(\sum_{j=1}^i c_{ij} v_j^{\mathsf{T}}\right) M_i \left(\sum_{j=1}^i c_{ij} v_j\right) = \sum_{j=1}^i c_{ij}^2 v_j^{\mathsf{T}} M_i v_j + \sum_{j \le i} \sum_{j \ne \ell \le i} c_{ij} c_{i\ell} v_j^{\mathsf{T}} M_i v_\ell.$$

Thus we find a lower bound on the difference of interest:

$$\sum_{i=1}^{k} \lambda_{i}(M) - \sum_{i=1}^{k} \lambda_{1}(M_{i}) \geq \sum_{i=1}^{k} \left(\sum_{j=1}^{i} (1 - c_{ij}^{2}) v_{j}^{\mathsf{T}} M_{i} v_{j} - \sum_{j \leq i} \sum_{j \neq \ell \leq i} c_{ij} c_{i\ell} v_{j}^{\mathsf{T}} M_{i} v_{\ell} \right)$$

and the first assertion would follow if we show that the terms in the brackets are non-negative. But according to the constraints on c_{ij} we have

$$\sum_{j=1}^{i} (1 - c_{ij}^2) v_j^{\mathsf{T}} M_i v_j = \sum_{j \le i} \sum_{j \ne \ell \le i} c_{i\ell}^2 v_j^{\mathsf{T}} M_i v_j$$

and it is left to check non-negativity of the terms

$$\sum_{j \le i} \sum_{j \ne \ell \le i} \left(c_{i\ell}^2 v_j^{\mathsf{T}} M_i v_j - c_{ij} c_{i\ell} v_j^{\mathsf{T}} M_i v_\ell \right) = \sum_{1 \le \ell < j \le i} \left(c_{i\ell} v_j - c_{ij} v_\ell \right)^{\mathsf{T}} M_i \left(c_{i\ell} v_j - c_{ij} v_\ell \right),$$

which is true due to assumed non-negative definiteness of all M_i , and the first assertion is proven.

The second assertion follows by taking the matrices

$$M_i = Q \operatorname{diag}(0, \dots, 0, \lambda_i(M), 0, \dots, 0) Q^{\mathsf{T}}, \quad 1 \leq i \leq k - 1,$$

$$M_k = Q \operatorname{diag}(0, \dots, 0, \lambda_k(M), \lambda_{k+1}(M), \dots, \lambda_d(M)) Q^{\mathsf{T}},$$

where Q is an orthogonal matrix in the diagonalization of M. Indeed, the matrices M_i are non-negative definite summing up to M, and the largest eigenvalues are $\lambda_i(M)$ for $i \leq k$.

APPENDIX B. HÜSLER-REISS DISTRIBUTION

Random generation of variogram. A d-dimensional max-stable Hüsler–Reiss distribution [Hüsler and Reiss, 1989] is parameterized by a conditionally negative definite $d \times d$ matrix Γ , called a variogram. Every such matrix has a representation $\Gamma_{ij} = ||h_i - h_j||_2^2$, where h_1, \ldots, h_d are the elements of some Hilbert space with norm $||\cdot||_2$, and every such construction yields a conditionally negative definite matrix, see [Vakhania et al., 1980, Property (g), p. 191]. As usual, we impose a further non-degeneracy assumption that Γ is strictly conditionally negative definite so that the associated exponent measure has a density [Engelke et al., 2015].

Suppose that Y has a max-stable Hüsler–Reiss distribution. Our main assumption requires a partition $I_1 \cup I_2 = \{1, \ldots, d\}$ of the index set such that $\chi_{ij} = \chi_{ji} = 0$ for all $i \in I_1$ and $j \in I_2$, which is equivalent to (asymptotic) independence of the two groups of components of Y. Recall the formula for the bivariate tail dependence coefficient:

$$\chi_{ij} = 2\overline{\Phi}(\sqrt{\Gamma_{ij}}/2),$$

where $\overline{\Phi}$ is the survival function of the standard normal distribution, and note that $\chi_{ij} = 0$ is obtained in the limit case $\Gamma_{ij} = \infty$. In practice, large entries in the respective locations of Γ would suffice, because of weak convergence of the respective distributions.

In our experiments we randomly generate Γ for d=100 according to the following procedure based on the aforementioned representation. Firstly, we generate d-dimensional vectors h_1, \ldots, h_d with i.i.d. Pareto distributed components having shape parameter 2.5. Secondly, we add one more dimension by letting

$$\widetilde{h}_i = \begin{cases} (h_i, L), & \text{if } i \le |I_1|, \\ (h_i, 0), & \text{if } i > |I_1|, \end{cases}$$

where $L = 10^5$ is a fixed large number. Then the variogram matrix Γ is set to $\frac{3}{d}(\|\widetilde{h}_i - \widetilde{h}_j\|_2^2)_{ij}$, where 3/d provides a scaling resulting in a suitable distribution of the tail dependence coefficients. Note that this procedure ensures that $\Gamma_{ij} \geq L$ for i and j in different groups.

Finally, we use the R package [Engelke et al., 2019] to sample vectors Y from the Hüsler–Reiss distribution specified by Γ . Note that $Y/\|Y\|_2$ given $\|Y\|_2 > t$ for a finite threshold t provides only an approximation of the limiting angle. The distribution of the exact angle is addressed below.

The angular distribution and the matrix Σ . Even though the exact matrix $\Sigma = E(XX^{\mathsf{T}})$ is not required for the simulation experiments, it can be used to verify the sufficient conditions in our main result. Below we determine the probability density function of X (with respect to the Euclidean norm) and provide an expression for Σ in terms of expectations of transformed Gaussian vectors.

As in [Engelke et al., 2015] we consider the $(d-1) \times (d-1)$ covariance matrix

$$R = \left\{ \frac{1}{2} \left(\Gamma_{id} + \Gamma_{jd} - \Gamma_{ij} \right) \right\}_{i,j \neq d}.$$

For all i = 1, ..., d we define the transformation

$$t_i(x) = \log(x_i/x_d) = \log\left(x_i/\sqrt{1 - x_1^2 - \dots - x_{d-1}^2}\right), \qquad x \in \text{int}(\mathbb{S}_+^{d-1}),$$
 (20)

where $\operatorname{int}(\mathbb{S}^{d-1}_+)$ stands for the simplex interior, and note that $t:\operatorname{int}(\mathbb{S}^{d-1}_+)\to\mathbb{R}^{d-1}$ is a bijection with the inverse

$$t^{-1}(z) = \frac{(\exp(z_1), \dots, \exp(z_{d-1}), 1)^{\top}}{\sqrt{1 + \exp(2z_1) + \dots + \exp(2z_{d-1})}}.$$

It turns out that each column of the matrix Σ/μ corresponds (up to a permutation) to $E(t^{-1}(Z))$ for a multivariate normal Z as specified below. The means and other moments of X can be obtained in a similar way.

Lemma B.1. For the d-dimensional Hüsler–Reiss distribution with the variogram Γ the density of the Euclidean angle (X_1, \ldots, X_{d-1}) is given by

$$f(x_1, \dots, x_{d-1}) = \mu x_d^{-2} \prod_{i \le d} x_i^{-1} \phi_{d-1}(t_1(x), \dots, t_{d-1}(x)), \qquad x \in \text{int}(\mathbb{S}_+^{d-1}), \tag{21}$$

where $\mu = EX_1$ and ϕ_{d-1} is the density of a multivariate normal distribution with covariance matrix R and mean vector $-(\Gamma_{1d}, \dots, \Gamma_{d-1,d})^{\top}/2$. Furthermore, letting g be the density of (W_1, \dots, W_{d-1}) where $W = t^{-1}(Z) \in \mathbb{S}^{d-1}_+$ and $Z \sim \phi_{d-1}$, there are the identities:

$$f(x_1, \dots, x_{d-1}) = \mu g(x_1, \dots, x_{d-1})/x_d,$$

$$\mu^{-1} = E(W_d^{-1}), \quad E(X_i X_d) = \mu E(W_i), \quad i = 1, \dots, d.$$

Proof. From [Engelke et al., 2015] it is known that the exponent measure has the density

$$\lambda(y) = y_d^{-1} \prod_{i < d} y_i^{-1} \phi_{d-1}(\log(y_1/y_d), \dots, \log(y_{d-1}/y_d)), \qquad y_1, \dots, y_d > 0.$$

We note that for the polar coordinates

$$y_1 = rx_1, \quad y_2 = rx_2, \quad \dots, \quad y_d = r(1 - x_1^2 - \dots - x_{d-1}^2)^{1/2},$$

the absolute value of the Jacobian evaluates to r^{d-1}/x_d , and so in these coordinates the density becomes

$$r^{-2}x_d^{-2}\prod_{i\leq d}x_i^{-1}\phi_{d-1}(t_1(x),\ldots,t_{d-1}(x)).$$

This must factorize into $r^{-2}f(x_1,\ldots,x_{d-1})/\mu$ according to [Resnick, 2008, Prop. 5.11(iv)] and the first result follows.

Let us compute the Jacobian $J_t(x)$ of the transformation t(x) defined in (20) and restricted to the first d-1 values. We have

$$\frac{\partial t_i}{\partial x_j}(x) = \frac{x_j}{s}, \quad j \neq i, \quad \text{and} \quad \frac{\partial t_i}{\partial x_i}(x) = \frac{x_i^2 + s}{x_i s},$$

where $s = 1 - x_1^2 - \dots - x_{d-1}^2 = x_d^2$, and so

$$J_{t}(x) = \begin{vmatrix} \frac{x_{1}^{2} + s}{x_{1}s} & \frac{x_{2}}{s} & \dots & \frac{x_{d-1}}{s} \\ \frac{x_{1}}{s} & \frac{x_{2}^{2} + s}{x_{2}s} & \dots & \frac{x_{d-1}}{s} \\ \vdots & \vdots & \ddots & \vdots \\ \frac{x_{1}}{s} & \frac{x_{2}}{s} & \dots & \frac{x_{d-1}^{2} + s}{x_{d-1}s} \end{vmatrix} = \frac{x_{1} \cdots x_{d-1}}{s^{d-1}} \begin{vmatrix} \frac{s}{x_{1}^{2}} + 1 & 1 & \dots & 1 \\ 1 & \frac{s}{x_{2}^{2}} + 1 & \dots & 1 \\ \vdots & \vdots & \ddots & \vdots \\ 1 & 1 & \dots & \frac{s}{x_{d-1}^{2}} + 1 \end{vmatrix}.$$

Using formula (1) in [Goberstein, 1980], we find that the last determinant is equal to

$$\frac{s^{d-1}}{x_1\cdots x_{d-1}} + \frac{s^{d-1}}{x_1\cdots x_{d-1}} \cdot \left(\frac{x_1^2}{s} + \cdots + \frac{x_{d-1}^2}{s}\right) = \frac{1}{x_1\cdots x_{d-1}s}.$$

Thus we have the relation $g(x) = (x_1 \dots x_{d-1}s)^{-1}\phi_{d-1}(t(x))$, where x and t(x) are restricted to the first d-1 elements. Comparing it with f, we indeed find the stated relation between f and g. Finally, observe that

$$E(X_i X_d) = \mu \int x_i g(x) dx = \mu E(W_i), \qquad 1 = \mu E(W_d^{-1}),$$

and the proof is complete.

The above result states that the last column of Σ/μ is given by the vector E(W). By changing the indexing we may easily find the other columns. In particular, in the bivariate case with parameter $\gamma = \Gamma_{12}$ we have

$$W_1 = [1 + \exp(-2\sqrt{\gamma}Z_0 + \gamma))]^{-1/2}, \qquad W_2 = (1 - W_1^2)^{1/2} = [1 + \exp(2\sqrt{\gamma}Z_0 - \gamma))]^{-1/2},$$

where Z_0 is a standard normal. Sadly, the moments $w_1 = E(W_1), w_2 = E(W_2)$ are not explicit, and the same applies to the matrix $\Sigma/\mu = \begin{pmatrix} 1-w_2 & w_1 \\ w_1 & w_2 \end{pmatrix}$.

References

[Chautru, 2015] Chautru, E. (2015). Dimension reduction in multivariate extreme value analysis. *Electron. J. Stat.*, 9(1):383–418.

[Chiapino et al., 2019] Chiapino, M., Sabourin, A., and Segers, J. (2019). Identifying groups of variables with the potential of being large simultaneously. *Extremes*, 22:193–222.

[Cooley and Thibaud, 2019] Cooley, D. and Thibaud, E. (2019). Decompositions of dependence for high-dimensional extremes. *Biometrika*, 106(3):587–604.

[Davison and Huser, 2015] Davison, A. and Huser, R. (2015). Statistics of extremes. Ann. Rev. Stat. App., 2:203–235.

[Davison et al., 2013] Davison, A. C., Huser, R., and Thibaud, E. (2013). Geostatistics of dependent and asymptotically independent extremes. *Math. Geosci.*, 45(5):511–529.

[Dhillon and Modha, 2001] Dhillon, I. S. and Modha, D. S. (2001). Concept decompositions for large sparse text data using clustering. *Machine learning*, 42(1-2):143–175.

[Drees and Sabourin, 2019] Drees, H. and Sabourin, A. (2019). Principal component analysis for multivariate extremes. arXiv:1906.11043.

[Engelke and Hitz, 2020] Engelke, S. and Hitz, A. S. (2020). Graphical models for extremes. J. R. Stat. Soc. B., 82(4):871–932.

[Engelke et al., 2019] Engelke, S., Hitz, Α. S., and Gnecco, Ν. (2019).GraphicalStatisticalMethodologyforExtremeValueModels.Available https://CRAN.R-project.org/package=graphicalExtremes, R package version 0.1.0.

[Engelke and Ivanovs, 2020] Engelke, S. and Ivanovs, J. (2020). Sparse structures for multivariate extremes. Ann. Rev. Stat. App. arXiv:2004.12182 (to appear).

[Engelke et al., 2015] Engelke, S., Malinowski, A., Kabluchko, Z., and Schlather, M. (2015). Estimation of Hüsler–Reiss distributions and Brown–Resnick processes. J. R. Stat. Soc. B., 77(1):239–265.

[Fan, 1949] Fan, K. (1949). On a theorem of Weyl concerning eigenvalues of linear transformations I. *Proceedings of the NAS of the USA*, 35(11):652.

[Gan et al., 2007] Gan, G., Ma, C., and Wu, J. (2007). *Data clustering*, volume 20. SIAM and ASA. Theory, algorithms, and applications.

[Goberstein, 1980] Goberstein, S. M. (1980). Evaluating "uniformly filled" determinants. Col. Math. J., 19(4):343–345.

[Goix et al., 2016] Goix, N., Sabourin, A., and Clémençon, S. (2016). Sparse representation of multivariate extremes with applications to anomaly ranking. In *Proceedings of the 19th International Conference on Artificial Intelligence and Statistics (AISTATS)*. JMLR: W&CP.

[Goix et al., 2017] Goix, N., Sabourin, A., and Clémençon, S. (2017). Sparse representation of multivariate extremes with applications to anomaly detection. *J. Multivar. Anal.*, 161:12–31.

[Hüsler and Reiss, 1989] Hüsler, J. and Reiss, R.-D. (1989). Maxima of normal random vectors: between independence and complete dependence. *Stat. Prob. Let.*, 7(4):283–286.

[Janssen and Wan, 2020] Janssen, A. and Wan, P. (2020). k-means clustering of extremes. Electron. J. Stat., 14:1211–1233.

[Larsson and Resnick, 2012] Larsson, M. and Resnick, S. I. (2012). Extremal dependence measure and extremogram: the regularly varying case. *Extremes*, 15:231–256.

[Meyer and Wintenberger, 2019] Meyer, N. and Wintenberger, O. (2019). Sparse regular variation. arXiv:1907.00686.

[Overton and Womersley, 1992] Overton, M. L. and Womersley, R. S. (1992). On the sum of the largest eigenvalues of a symmetric matrix. SIMAX, 13(1):41–45.

[Palarea-Albaladejo et al., 2012] Palarea-Albaladejo, J., Martín-Fernández, J. A., and Soto, J. A. (2012). Dealing with distances and transformations for fuzzy c-means clustering of compositional data. J. Classif., 29(2):144–169.

[Resnick, 2008] Resnick, S. I. (2008). Extreme Values, Regular Variation and Point Processes. Springer, New York.

[Simpson et al., 2018] Simpson, E., Wadsworth, J., and Tawn, J. (2018). Determining the dependence structure of multivariate extremes. arXiv:1809.01606.

[Vakhania et al., 1980] Vakhania, N. N., Tarieladze, V. I., and Chobanyan, S. A. (1980). *Probability Distributions on Banach Spaces*. Mathematics and Its Applications (Soviet Series). D. Reidel Publishing Company.

[Wang et al., 2018] Wang, J., Wang, W., Garber, D., and Srebro, N. (2018). Efficient coordinate-wise leading eigenvector computation. In *Algorithmic Learning Theory*, pages 806–820. PMLR.